Online optimal control of a parallel hybrid with after-treatment constraint integration

Alexandre Chasse, Gilles Corde and Alessio Del Mastro
IFP, 1 et 4, avenue de Bois-Préau,
92852 Rueil-Malmaison Cedex –France
alexandre.chasse@ifp.fr

Florent Perez
D2T, 11, rue Denis Papin
78190 TRAPPES

***Abstract*-The present paper deals with the activities and the results achieved under a cooperative research project between IFP, D2T, LMS, G2Elab and Renault focused on Hardware-in-the-Loop (HIL) applications to hybrid power-trains conception and assessment. The main goal of this study is the evaluation of hybrid propulsion concepts and the benefits of different degrees of hybridization in a flexible architecture, by using a chain of simulation platforms: from the co-simulation to the high-dynamic engine-in-the-loop test bed, through a virtual version of the last one. This paper focuses on the implementation issues of an energy management strategy (EMS) for a parallel hybrid architecture. The EMS is developed from the optimal control theory, using Pontryagin's Minimum Principle (PMP). The resulting Equivalent Consumption Minimization Strategy (ECMS) is implemented in real time and tested in an experimental environment (HyHiL test bench). In particular, a possible integration of the three way catalytic converter constraint in the optimization is presented.**

I. INTRODUCTION

NOWADAYS hybrid propulsion systems are increasingly recognized as one of the few possibilities of combining low carbon dioxide emissions, acceptable range, and good performance in road vehicles. In spite of their complexity with respect to conventional powertrains, hybrids offer additional degrees of freedom that can be optimized.

Optimization of hybrid energy management (supervisory control) ensures that the hybrid operation along, e.g., a drive cycle, is optimal with respect to some dynamic criterion, typically related to energy consumption, subjected to several constraints. The optimization and control of hybrid powertrains is increasingly based on system modeling, in contrast to heuristic strategies dictated by experience only. Model-based techniques are inherently more flexible than heuristic strategies and they can fully exploit the potential for energy consumption reduction. The literature offers several examples concerning parallel hybrids [1], but also series [2], and combined hybrids [3, 4]. Many of these examples develop a control law (Equivalent Consumption Minimization Strategy, ECMS) based on the formulation of an optimal control problem. Usually the optimality criterion is the fuel consumption (and possibly local pollutant emissions), with the main constraint on battery charge-sustaining operation. One often hidden assumption is that HEV system is under thermal equilibrium. However, thermal transients are in HEVs even more important than in conventional engine-propelled vehicles, since the engine itself is subject to stop-and-start phases and engine temperature has an influence on local emission and fuel consumption rates. Few publications have reported researches aimed at integrating Thermal Management Strategies (TMS) in the more general framework of EMS. Some steps toward the management of the three way catalytic converter temperature in the framework of an optimal EMS are reported in this paper and in the companion paper [5]. The latter focuses on integrating the engine temperature as a state variable in the EMS.

The paper is organized as follows. Section II describes the system model. The nominal optimal control laws are presented in Section III, alongside with a study on the effect of small heuristic modification for the gasoline after-treatment activation. Section IV describes the after-treatment model used for the optimization with some experimental results. Section V presented the integration of this model in the EMS.

II. SYSTEM DESCRIPTION AND MODELING

A. *System description*

The parallel hybrid architecture analyzed in this paper is depicted in Figure 1.

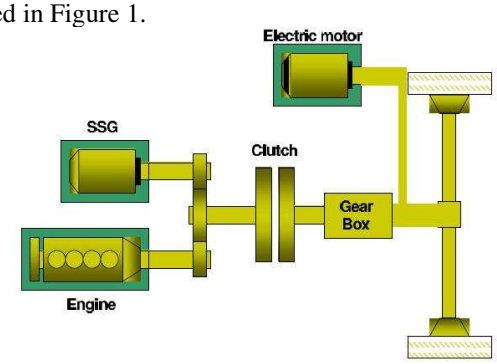

Fig. 1. The parallel hybrid architecture analyzed

The engine is a gasoline turbocharged engine. The pre-transmission electric machine is a starter-generator (SSG) that is only allowed to start the engine in this application, without any boosting or regenerating capabilities. In contrast, the post-transmission electric machine (MOT) allows for power assist, including purely electric drive, and battery recharge, including regenerative braking. The transmission ratio between the electric machine and the wheels is constant, while the gearbox is an automated manual transmission.

978-1-4244-8218-4/10/$26.00 ©2010 IEEE

B. System modeling

A backward model of the parallel hybrid vehicle described above is developed to serve as a basis for the optimization and to capture the dominant dynamic effects [6].

1) Model of the transmission: In backward modeling, the driver's torque demand and the vehicle speed are the principal inputs of the model. The former is calculated from the position of the acceleration and brake pedals. The resulting value $T_{pwt\_sp}(t)$ can be positive (traction) or negative (braking).

This torque demand has to be split between the engine and the electric motor. A control input can be set as $u(t) = T_{eng}(t)$, the engine torque. The requested electric motor torque $T_{mot}(t)$ for a given gearbox ratio $R_{gb}(t)$ is then determined as

$$T_{mot}(t) = \frac{T_{pwt\_sp}(t) - R_{gb}(t) \cdot T_{eng}(t)}{R_1} \tag{1}$$

where R_1 is the constant motor-to-wheels transmission ratio.

2) Model of the engine: The fuel consumption of the engine is given by a steady-state map as a function of engine torque T_{eng} and engine speed ω_{eng},

$$\dot{m}_{fuel}(t) = f_1(T_{eng}, \omega_{eng}) \tag{2}$$

The power consumed with the fuel can be computed from the latter expression and the fuel lower heating value H_f,

$$P_{fuel}(t) = H_f \cdot \dot{m}_{fuel}(t) \tag{3}$$

3) Model of the traction motor: The electric motor power P_{ele} is given by a steady-state map as a function of the motor torque T_{mot} and the motor speed ϖ_{mot},

$$P_{ele}(t) = f_2(T_{mot}, \omega_{mot}) \tag{4}$$

4) Model of the traction battery: Batteries are often represented in system-level simulators as simple equivalent circuits. The equivalent electric circuit comprises a voltage source U_{oc} and a resistance R_i in series, both varying with the state of charge $\xi(t)$. The resulting equation

$$U_{bat}(t) = U_{oc}(\xi(t)) - R_i(\xi(t)) \cdot I_{bat}(t) \tag{5}$$

relates two unknowns, the battery current I_{bat} and voltage U_{bat}. A second equation is given by the battery power definition, $P_{bat} = I_{bat} \cdot U_{bat}$. Thus, the current is calculated as

$$I_{bat}(t) = \frac{U_{oc}}{2R_i} - \sqrt{\frac{{U_{oc}}^2}{4R_i^2} - \frac{P_{bat}(t)}{R_i}} \tag{6}$$

Combining (6) with the energy conservation at the DC bus level, the battery current can be expressed as a function of P_{ele} and ξ,

$$I_{bat}(t) = f_3(P_{bat}, \xi) = f_3(P_{ele}, \xi) \tag{7}$$

The variation of the battery state of charge (SOC) is calculated from the battery current and power:

$$\dot{\xi}(t) = \begin{cases} -I_{bat}(t)/Q_O, & P_{bat} > 0 \\ -\eta_{bat}(\xi) \cdot I_{bat}(t)/Q_O, & P_{bat} < 0 \end{cases} \tag{8}$$

where Q_0 is the battery capacity and η_{bat} is its Faradic efficiency.

The inner (electrochemical) battery power is finally calculated as

$$P_{ech}(t) = -\dot{\xi}(t) \cdot Q_0 \cdot U_{oc}(\xi(t)) \tag{9}$$

III. HYBRID OPTIMIZATION PROBLEM

The optimization goal is to develop a torque split strategy in order to minimize a certain global criterion under certain local and global constraints. In this paper, we will focus on the on-line optimization. This optimizer runs in real time on board of the vehicle and thus it has no a priori knowledge of the future drive cycle (torque request). It will be referred to as energy management system.

1) Mathematical formulation

In the formulation of this paper, the global criterion is the overall fuel consumption and the global constraint is on the final state of charge of the battery, which has to match the value at the beginning of the cycle. Considering the model of Sect. II.B, this optimal control problem is stated as [7]

$$\begin{cases} \min\limits_{u \in U} \left\{ J(u) := \int_0^T \dot{m}_{fuel}(u(t), t) dt \right\} \\ \dot{\xi}(t) = f(\xi(t), u(t), t), \quad with \quad \xi(T) = \xi(0) \end{cases} \tag{10}$$

where the controlled variable is the engine torque and U is the space of admissible controls. The problem is solved using Pontryagin's Minimum Principle (PMP),

$$u^0(t) = \arg\min H(\xi(t), u(t), t) \tag{11}$$

where the superscript 0 denotes optimal trajectories, the Hamiltonian function is defined as

$$H(t) = \dot{m}_{fuel}(u(t), t) + \lambda^0(t) \cdot \dot{\xi}(u(t), t) \tag{12}$$

and λ^0 is the co-state of SOC. Equation (12) can be reformulated in more physical terms as

$$H'(\xi(t),u(t),t,s(t)) = P_{fuel}(u(t),t) + s^0(t)\cdot P_{ech}(\xi(t),u(t),t) \quad (13)$$

The equivalence factor $s(t)$ that weights the electrochemical power before summing it to the fuel power is proportional to the costate, as shown by (9). The corresponding Euler-Lagrange equation shows that, if the dependency of H on ξ is negligible, s^0 is a constant during the drive cycle. This constant value s^0 is such that the condition $\xi(T) = \xi(0)$ is fulfilled. Under this assumption, a suboptimal control law is found generally as

$$u^0(t) = \arg\min\left\{P_{fuel}(u(t),t) + s^0 \cdot P_{ech}(\xi(t),u(t),t)\right\} \quad (14)$$

The latter equation corresponds to the minimization of a cost function that depends only on the current driving conditions and on s^0.

2) Equivalence factor expression: Using a constant equivalence factor s^0 is only possible if the entire cycle is known in advance (off-line optimization case). In the on-line optimization case, a constant equivalence factor cannot be used since its value is not known a priori. Thus, any open-loop guess of s^0 would result in a deviation from the optimal trajectory.

Thus, one possibility to proceed consists in continuously estimate the value s^0 as a function of the state of charge deviations. Some expressions for this online-adapted equivalence factor can be found, e.g., in [8, 9]. The adaptation law used here [10] is a simple expression between the equivalence factor and the state of charge,

$$s(t) = s_{opt} + K_p \cdot (\xi_{sp} - \xi(t)) + K_I \cdot \int (\xi_{sp} - \xi(t))dt \quad (15)$$

where ξ_{sp} is a setpoint for the state of charge and ξ is here the SOC measurement or estimation. The three tuning parameters of (15) are s_{opt}, the two gains K_p and K_I. The parameter s_{opt} is the open-loop component of the estimation. It can be calculated from off-line optimization and it is specific of the drive cycle. The proportional gain K_p must be calibrated to avoid that the variations of SOC exceed the admissible SOC range. The integral gain K_I must be calibrated to compensate the estimation error on the open loop component s_{opt}. This integral term has the rule of cycle-independent calibrations of the control parameters. In our case this parameter K_I is equal to zero since the parameter s_{opt} is computed for the same driving cycle.

3) Limitation of this formulation: The previous formulation of the optimization problem has been validated using simulation and experimental tools on different driving cycles with a hot initial thermal state of the engine and the after treatment system. In this condition the effectiveness of the three-way catalytic converter is maximal and all the principal pollutants are converted. These first tests are necessary for the control of the state of charge but the impact on the pollutants emissions are not taking into account. In order to quantify this effect, the same driving cycles have been realized in the conventional initial thermal conditions (engine at 25°C).

The table 1 shows the results obtained on the experimental tool (HiL hybrid test bench) [13, 14]. The table compares the reduction of the fuel consumption and the pollutant emissions measured on a NEDC driving cycle. The first line represents the results of the conventional vehicle without hybrid components. The second line (Full hybrid without warm-up strategy) represents the results obtained with the EMS presented in the previous. These first results shows the importance of the integration of a warm up strategy for the after treatment system since the fuel consumption has been reduce to the detriment of the pollutants emissions (HC and CO).

	FC & Pollutant emissions [%]			
	Fuel Consumption	HC	CO	NOx
Conventional	100	100	100	100
Full hybrid without warm-up strategy	68	276	168	35

Tab. 1. Pollutants emissions obtain on a NEDC driving cycle without a warm up strategy for the after treatment system

In order to reduce the fuel consumption and the pollutants emissions, two heuristic warm up strategies of he three way catalytic converter have been tested. These two heuristic warm up strategies implemented (strategy H1 and H2) are based on water coolant temperature thresholds. Depending on the value of the water coolant temperature (Tcool), different operating modes are authorized. These two heuristic strategies are described below.

- Strategy Heuristic 1 (H1): No-Hybrid + Full-hybrid:
  - $T_{COOL} < 60°C \Rightarrow$ No-use of the electric motor (conventional mode)
  - $T_{COOL} > 60°C \Rightarrow$ Full-Hybrid mode (full electric authorized)

- Strategy Heuristic 2 (H2):: No-Hybrid + Micro-Hybrid + Full-Hybrid:
  - $T_{COOL} < 40°C \Rightarrow$ No-use of the electric motor (conventional mode)
  - $40°C < T_{COOL} < 60°C \Rightarrow$ Micro-Hybrid mode (full electric not authorized)
  - $T_{COOL} > 60°C \Rightarrow$ Full-Hybrid mode (full electric authorized)

	FC & Pollutant emissions [%]			
	Fuel Consumption	HC	CO	NOx
Conventional	100	100	100	100
Full hybrid with warm-up strategy H1	74	166	120	60
Full hybrid with warm-up strategy H2	73	150	113	57

Tab. 2. Experimental results of the impact of the warm-up strategy on the pollutants emissions on a NEDC driving cycle.

Table 2 resumes the results obtained with these two heuristic strategies on the experimental tool. Thanks to a simple warm up strategy, we arrive to reduce the pollutants emissions with a small increasing of the fuel consumption. These results clearly show that the management of the state of the engine has an important impact on the global pollutant emissions. These results are directly linked to the difference on the thermal evolution of the after-treatment system as shown on Fig 3. The pollutants are completely converted when the temperature of the catalytic converter is higher than 350 °C.

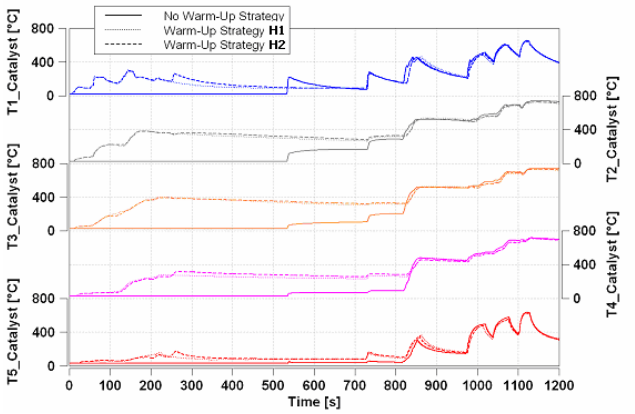

Fig. 3. After- treatment thermal evolution for the different warm-up strategy on a NEDC driving cycle.

Thanks to a simple warm up strategy with a real work of calibration, it's possible to reduce the pollutant emissions of this hybrid vehicle. But this work of calibration will be only valid on an NEDC driving cycle and the same work will make for another driving cycle. Consequently, the objective of the after-treatment integration in the EMS is to find the better trade-off between the fuel economy and pollutant emissions without calibration for a specific driving cycle. The thermal managing of the after-treatment device is realized on the basis of a specific catalyst model directly implemented on the EMS.

IV. SIMPLE THREE WAY CATALYTIC CONVERTER MODEL

This section highlights the equations that constitute the heart of the model. Moreover, this section briefly presents the results obtained with this model and compares them to experimental results. Different types of three-way catalytic converter models can be found in the literature [12, 13]. The main difference is the consideration of the position in the catalytic converter. In the model presented this dimension is not taken into account. The three-way catalytic converter is split into two parts considered as being homogeneous.

In order to develop the equation for the average gas temperature across an element, both the heat transfer rate equation and the conservation of energy for the gas stream are required. The heat transfer, found from the difference between the gas and the average wall temperature begins the derivation process by providing the following equation.

$$\dot{m}_g \cdot C_{p_g} \cdot \frac{\partial T_g}{\partial z} = -h_I \cdot P_{I_{cat}} \left(T_g - T_w \right) \tag{16}$$

With $\dot{m}_g$ the exhaust mass flow rate, C_{p_g} the heat capacity of the exhaust gas, h_I the internal heat transfer coefficient, $P_{I_{cat}}$ the total catalyst cell inside perimeter, T_g and T_w are the gas and wall temperatures, respectively.

After the integration of this equation on the element, the gas temperature at the output $T_{g,l}$ of an element becomes.

$$T_{g,l} = T_{g,0} - \beta_0 \left(\beta_1 \cdot T_{g,0} - \beta_2 \cdot T_w \right) \tag{17}$$

With $T_{g,0}$ the exhaust gas at the input of the catalyst system.

The effects of thermal mass and convective heat transfer (between the gas and wall, and between the wall and atmosphere, plus thermal conduction along the wall) on the gas and wall temperature are determined using the conservation of energy for the surface.

$$\begin{cases} \left(m \cdot c_p \right)_s \cdot dT_s = dh_{tot} + dh_{reac} + dh_{\text{int}} \\ dh_{tot} = H_{tot} \cdot A \cdot \left(T_{air} - T_s \right) \\ dh_{\text{int}} = \dfrac{4 \cdot H_{\text{int}}}{D_{ch}} \cdot V \cdot \left(T_g - T_s \right) \end{cases} \tag{18}$$

With dh_{reac} corresponding to the heat due to pollutants conversion and transferred to the monolith, dh_{int} corresponding to the convective heat exchange between the monolith channels and the internal flow and dh_{tot} corresponding to the conduction through the insulated casing and convective exchange between the catalytic converter and the ambient air.

This model has been calibrated and compared to experimental results as shown on Figure 4. This figure shows the evolution of the gas temperature in the first element of the three-way catalytic converter. This result confirms that the model used is sufficient for the integration in the optimization need. Moreover the pollutant emissions downstream of the

three-way catalytic converter are sufficiently accurate to be used for the control.

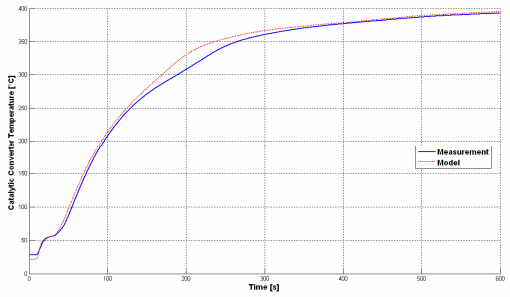

Fig. 4. Comparison of the three-way catalytic converter gas temperature evolution for experimental and simulation results.

V. INTEGRATION OF THE THREE WAY CATALYTIC CONVERTER MODEL IN THE OPTIMIZATION

As shown in section IV, the formulation of the global criterion on the fuel consumption is not sufficient for the cold engine condition, thus an adaptation with the pollutants emissions is necessary. The new global criterion is the sum of the overall CO2 emissions and the principal regulated pollutants (HC, CO and NOx). The global constraint is always on the final state of charge of the battery, which has to match the value at the beginning of the cycle. This optimal control problem is stated as

$$\begin{cases} \min\limits_{u\in U}\left\{ J(u) := \int_0^T (\dot{m}_{CO_2} + \alpha_1 \cdot \dot{m}_{HC} + \alpha_2 \cdot \dot{m}_{NO_x} + \alpha_3 \cdot \dot{m}_{CO})dt \right\} \\ \dot{\xi}(t) = f_1(\xi(t), u(t), t), \quad with \quad \xi(T) = \xi(0) \\ \dot{T}_{cat}(t) = f_2(T_{cat}(t), u(t), t) \end{cases} \tag{19}$$

Where $\dot{T}_{cat}$ is the temperature in the three way catalytic converter.

The problem is also solved using Pontryagin's Minimum Principle (PMP),

$$u^0(t) = \arg\min H(\xi(t), u(t), t) \tag{20}$$

where the superscript 0 denotes optimal trajectories, the Hamiltonian function is defined as

$$H(t) = \dot{m}_{pollutants}(u(t),t) + \lambda_1(t) \cdot \dot{\xi}(u(t),t) + \lambda_2(t) \cdot \dot{T}_{cat}(u(t),t) \tag{21}$$

with λ_1 the co-state of SOC and λ_2 the co-state of three way catalytic converter temperature.

Where

$$\dot{m}_{pollutants} = \dot{m}_{CO_2} + \alpha_1 \cdot \dot{m}_{HC}(T_{cat}) + \alpha_2 \cdot \dot{m}_{NO_x}(T_{cat}) + \alpha_3 \cdot \dot{m}_{CO}(T_{cat}) \tag{22}$$

$\dot{m}_{pollutants}$ represents the combination of the different pollutants downstream the after-treatment system. It is computed with different coefficients α_1, α_2 and α_3 that can be used to take into account a specific pollutant species reduction or a compromise between different species. The different species mass flows upstream of the three-way catalytic converter are obtained from the simplified after-treatment model (efficiency conversion for a specific temperature) and the upstream pollutant emissions are given by a map (obtained from the steady-state point operated on the test bed).

As seen before for the equation (12), the equation (21) can be reformulated in more physical terms as

$$\begin{aligned} H'(\xi(t), u(t), t, s(t)) &= P_{pol}(T_{cat}(t), u(t), t) \\ &+ s^0(t) \cdot P_{ech}(\xi(t), u(t), t) \\ &+ p^0(t) \cdot P_{th}(T_{cat}(t), u(t), t) \end{aligned} \tag{23}$$

With $P_{pol}(T_{cat}(t), u(t), t)$ the pollutants "power" compute from $\dot{m}_{pollutants}$ and the lower heating value of the fuel, $P_{ech}(\xi(t), u(t), t)$ the battery inner electrochemical power and $P_{th}(T_{cat}(t), u(t), t)$ the thermal power given to the catalytic converter. Thanks to this reformulation of the Hamiltonian, the expression of the Hamiltonian is similar to the previous without the integration of the catalytic converter constraint. The equivalence factor $s(t)$ that weights the electrochemical power before summing it to the fuel power is proportional to λ_1 the co-state of SOC, and $p(t)$ a factor that is proportional to λ_2 the co-state of three way catalytic converter temperature.

In our case the value of the equivalent factor $s(t)$ is taken as a constant and the second one factor $p(t)$, related to the catalyst temperature dynamics computed from the corresponding Euler-Lagrange equation [7]:

$$\dot{\lambda}_2(t) = -\frac{\partial H}{\partial T_{cat}}(u(t),t) \tag{24}$$

The explicit derivation of $\dot{p}(t)$ is cumbersome but straightforward, thus the details are not provided in this paper.

This modification of the criteria to be minimized has been integrated in the EMS for the simulation and the experimental tools.

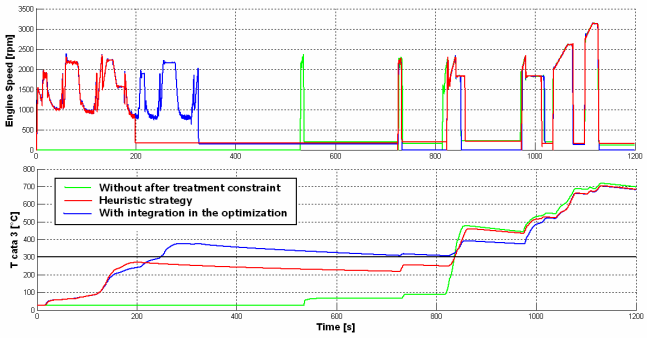

Fig. 5. Comparison of the engine speed and the temperature in the second monolith of the three ways catalytic converter on a NEDC driving cycle for three different strategies integration.

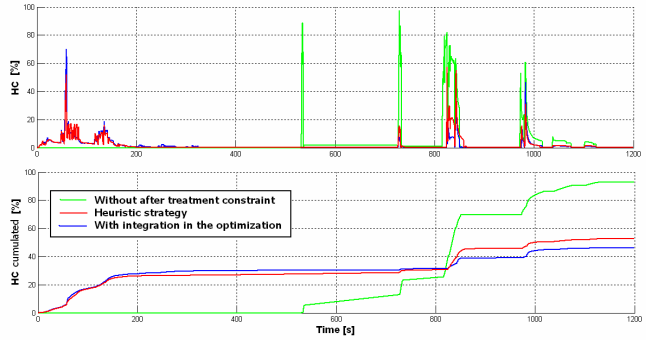

Fig. 6. Comparison of the instantaneous HC emissions and the cumulated HC emissions on a NEDC driving cycle for three different strategies integration.

Figure 5 and Figure 6 shows the results obtained on the experimental tool for the same NEDC driving cycle operated in the conventional initial thermal conditions (engine at 25°C) for three different warm-up strategies.

The first one is the baseline EMS strategy without the integration of the after treatment constraint. The second one is a heuristic strategy presented in the section III. The third one is a first result obtained with the integration of the after-treatment system in the optimization.

This figure clearly shows that the integration of this constraint ensures reducing the global pollutant emissions, which are lower than with the heuristic strategy. These results show the interest of the integration of this constraint. Another point to take into account is integration of the physical model of the after-treatment in the optimization that allows reducing the calibration of the warm up strategy on the real system.

Furthermore, the integration of the after-treatment constraint does not modify the behavior of the baseline EMS when the after-treatment system is activated (catalytic converter temperature higher than a specific value).

VI. Conclusion and Perspectives

This paper proposed a possible integration of the after-treatment constraint in the optimization of the power splitting on a hybrid vehicle.

The paper presented satisfying simulation results, and this adaptation is implemented in the real system described here. The first experimental results have shown that the proposed strategy has been successfully applied to this system and the integration of the after-treatment constraint does not modify the behavior of the previous EMS when the after treatment system is activated (catalytic converter temperature higher than a specific value).

In the perspectives, the authors proposed a simplify expression of the co-state λ_2 linked to the catalytic temperature dynamic to improve the integration in a EMS.

References

[1] A. Sciarretta, L. Guzzella, “Control of hybrid electric vehicles. Optimal energy-management strategies”, Control Systems Magazine, vol. 27, no. 2, April 2007, pp. 60-70.

[2] R. Cipollone, A. Sciarretta, “Analysis of the potential performance of a combined hybrid vehicle with optimal supervisory control”, Proc. of the IEEE International Conference on Control Applications, Munich, Germany, October 4-6, 2006 (invited paper).

[3] M. Anatone, R. Cipollone, A. Donati, A. Sciarretta, “Control-oriented modeling and fuel optimal control of a series hybrid bus”, SAE paper no. 2005-01-1163, 2005.

[4] J. Liu, H. Peng, “Control optimization for a power-split hybrid vehicle”, in Proc. of the American Control Conference, 2006

[5] J. Lescot, A. Sciaretta, Y. Chamaillard, A. Charlet, “On the integration of optimal energy management and thermal management of hybrid electric vehicles », VPPC 2010

[6] X. Wei, L. Guzzella, VI. Utkin, G. Rizzoni, “Model-based fuel optimal control of hybrid electric vehicle using variable structure control systems, Measurements and Control”, vol. 129, January 2007, no. 1, pp. 13-19.

[7] A.E. Bryson, H.C. Ho, Applied optimal control. John Wiley, New York. 1975.

[8] D. Ambühl, A. Sciarretta, C. Onder, L. Guzzella, S. Sterzing, K. Mann, D. Kraft, M. Küsell, “A causal operation strategy for hybrid electric vehicles based on optimal control theory”, 4th Symposium Hybrid Vehicles and Energy Management, Braunschweig, 2007.

[9] A. Kleimaier and D. Schröder, “An approach for the online optimized control of a hybrid powertrain”, in Proc. 7th Int. Workshop Advanced Motion Control, Maribor, Slovenia, 2002, pp. 215-220.

[10] A. Chasse, A. Sciarretta, and J. Chauvin, “Online optimal control of a parallel hybrid with costate adaptation rule,” *accepted for publication in 6th IFAC Symposium Advances in Automotive Control*, 2010

[11] A. Chasse, P. Pognant-Gros, A. Sciarretta, “Online Implementation of an Optimal Supervisory Control for a Parallel Hybrid Powertrain”, Florence, Italy, June 6-8, 2009.

[12] A. Chasse, G. Hafidi, P. Pognant-Gros, and A. Sciarretta, “Supervisory control of hybrid powertrains: an experimental benchmark of offline optimization ond online energy management,” *in Proc of the IFAC Workshop on Engine and Powertrain Control, Simulation and Modelling*, 2009.

[13] A. Lubeski, “Real-Time Catalytic Converter Temperature Estimator in the Powertrain Controller”, SAE, 2000-01-0651

[14] Paul M. Laing, Michael D. Shane, “A Simplified Approach to Modeling Exhaust System Emissions:SIMTWC”, SAE, 1999-01-3476